Robust String Stability and Safety of CTH Predictor-Feedback CACC

Nikolaos Bekiaris-Liberis, *Member, IEEE*

***Abstract*— We establish robustness of string stability to delay uncertainty as well as positivity of spacing and speed states, for homogeneous vehicular platoons under predictor-feedback Cooperative Adaptive Cruise Control (CACC). Each individual vehicle's dynamics are described by a second-order linear system with delayed desired acceleration, under acceleration information transmitted to the ego vehicle from a single, preceding vehicle. The nominal design (in the delay-free case) is a constant time-headway (CTH) policy and no restriction on the delay size, in relation with the desired time headway, is imposed. The proofs rely on combination of an input-output approach (on the frequency domain) and on deriving estimates on explicit, closed-loop solutions; under specific, sufficient conditions that are derived on initial conditions and parameters of the baseline, CTH controller. We illustrate in simulation and numerical examples, the guarantees of robust stability and string stability as well as of collisions avoidance, of CTH predictor-feedback CACC design. We also present extensions of our design and analysis approach to heterogeneous, third-order dynamic models of vehicles.**

***Index Terms*— Delay compensation, string stability of vehicular platoons, cooperative adaptive cruise control (CACC), predictor feedback, safety of vehicular platoons.**

I. Introduction

STRING stability and collisions avoidance of vehicular platoons are two of the primary objectives of ACC/CACC designs. Both, however, are jeopardized in the presence of actuator, sensor, and communication delays; see, for example, [14], [16], [24], [27], [31]. For this reason there exist ACC/CACC designs that aim at studying robustness of baseline control laws to small delays [11], [13], [16], [24], [35], [39], [41] and designs that aim at delay compensation of larger delays [10], [18], [25], [34], [36], [37], [38], [40].

Despite the existence of such ACC/CACC designs only the predictor-feedback CACC design in [10] provably guarantees individual vehicle stability and $\mathcal{L}_2$ string stability (and zero steady-state spacing error), under the minimum vehicle-to-vehicle (V2V) communication requirements and without imposing any limitation on the size of the delay, in relation with the desired time headway. This is also an important improvement compared to the ACC version of predictor feedback [6] that requires the delay to be smaller than the desired headway to guarantee string stability (and the addition of integral action to guarantee zero, steady-state spacing error). This advantage is a result of the fact that (besides predictor-feedback CACC inheriting predictor-feedback's properties [4] as regards closed loop performance) V2V communication enables construction of an implementable formula for the predictor state of the preceding vehicle's speed, which can be achieved employing acceleration measurements transmitted from the preceding vehicle. In fact, V2V communication is needed only for this reason and the underlying, delay-free design is of ACC type.

Although in [10] it is proved that the closed-loop, vehicular systems under predictor-feedback CACC are asymptotically stable and that the platoon is string stable in $\mathcal{L}_2$, neither a proof of positivity of spacing and speed states nor a proof of $\mathcal{L}_p$, $p \in [1, \infty]$, string stability are presented. In particular, $\mathcal{L}_\infty$ string stability implies non-overshooting speed response, due to preceding vehicle's speed variations (that can be guaranteed with a respective, non-negative impulse response), which cannot be guaranteed only via $\mathcal{L}_2$ string stability (see, for example, [6], [7], [8], [32]), thus implying improved safety and performance properties of the platoon, in response to leading vehicle's maneuvers. More importantly, no guarantee is provided that the spacing and speed states remain positive, despite the effect of initial conditions. Furthermore, as the only model parameter employed in the predictor-feedback CACC design is the delay value, which may be subject to uncertainty, it is significant to study robustness of string stability, under predictor-feedback CACC, to delay mismatches.

Building upon the design in [10] we establish $\mathcal{L}_\infty$ string stability of the platoon, positivity of spacing and speed states, and robustness of $\mathcal{L}_2$ string stability to delay mismatches. The proofs rely on a combination of an input-output approach and on deriving estimates on closed-loop solutions. Thus, it is proved that, for any size of the delay and time headway, CTH predictor-feedback CACC guarantees safety of the platoon, in the sense of guaranteeing i) stability of individual vehicles, ii) collisions avoidance, and iii) $\mathcal{L}_p$, $p \in [1, \infty]$, string stability. We also present the respective predictor-feedback CACC design and present proofs of positivity of speed/spacing states, as well as of stability and string stability accounting for heterogeneous a) third-order dynamics (to account, e.g., for engine dynamics), b) control parameters, and c) desired headways. We choose to focus on the computationally (and notationally) simpler, homogeneous second-order dynamics in the largest part of the paper in order to more clearly illustrate the main design and analysis ideas without distracting the

Manuscript received 10 May 2022; revised 14 December 2022; accepted 21 March 2023. Date of publication 12 April 2023; date of current version 2 August 2023. This work was supported by the Hellenic Foundation for Research and Innovation (H.F.R.I.) under the 2nd Call for H.F.R.I. Research Projects to Support Faculty Members and Researchers under Project 3537/ORAMA. The Associate Editor for this article was L. Du.

The author is with the Department of Electrical and Computer Engineering, Technical University of Crete, 73100 Chania, Greece (e-mail: bekiaris-liberis@ece.tuc.gr).

Digital Object Identifier 10.1109/TITS.2023.3265209

reader with tedious algebraic computations, as the extension to account for a)–c) is conceptually straightforward (even though computationally cumbersome). The theoretical guarantees derived are illustrated via numerical simulation and examples.

Notation and Definitions

The Laplace transform of a function $f(t)$, $t \geq 0$, is denoted by $F(s) = \mathscr{L}\{f(t)\}$. We denote by $\mathcal{L}_p$, $p \in [1, \infty]$, the temporal norm of a signal $f(t)$, $t \geq 0$.

An interconnected system of vehicles, indexed by $i = 1, \ldots, N$, following each other in single lane without passing, is $\mathcal{L}_p$ string stable if the following hold for $i = 2, \ldots, N$ (for initial conditions at equilibrium; see, e.g., [22] and [28])

$$\|\delta_i\|_p \leq \|\delta_{i-1}\|_p, \tag{1}$$

where $\delta_i = s_i - hv_i$, with spacing $s_i = x_{i-1} - x_i - l$, $i = 1, \ldots, N$, while x_j is the position of vehicle j and l is its length; v_i denotes the speed of vehicle i, $h > 0$ is the desired constant time-headway. We adopt the convention $v_0 = v_l$, where v_l is the speed of the string leader (see Fig. 1). On the way of studying string stability with respect to spacing error, we also establish string stability with respect to speed, since for homogeneous platoons the transfer function utilized, relating spacing error of the ego vehicle in response to spacing error variations of its preceding, is identical to the respective transfer function relating speed states variations. For heterogeneous vehicles (considered in Section VI) we study string stability with respect to speed and spacing error separately, as the respective transfer functions may be different.

II. Predictor-Feedback CACC for Homogeneous Platoons With Actuator Delay

A. Vehicle Dynamics

We consider a homogeneous string of vehicles (see Fig. 1) each one modeled by the following second-order linear system, with delayed desired acceleration, which is the manipulated variable (see, e.g., [13], [34])

$$\dot{s}_i(t) = v_{i-1}(t) - v_i(t), \tag{2}$$

$$\dot{v}_i(t) = u_i\,(t - D)\,, \tag{3}$$

$i = 1, \ldots, N$, where s_i and v_i are defined in Section I, u_i is the individual vehicle's control variable, $D \geq 0$ is actuator delay, and $t \geq 0$ is time. A uniform equilibrium point of systems (2), (3) is obtained when all vehicles have zero acceleration with speed dictated by a constant, leader's speed. For the leading vehicle's speed dynamics we assume similarly that $\dot{v}_l(t) = u_l(t - D)$, where $u_l \in C[-D, +\infty)$ is leader's desired acceleration, acting as exogenous input.

B. Delay-Free Control Design

Without actuator delay, the following CTH control strategy is used (see, e.g., [30])

$$u_i(t) = \alpha\left(\frac{s_i(t)}{h} - v_i(t)\right) + b\,(v_{i-1}(t) - v_i(t))\,, \tag{4}$$

where α and b are positive design parameters.

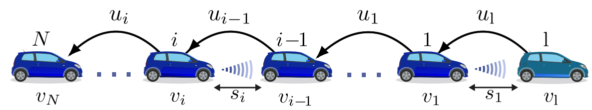

Fig. 1. Platoon of $N+1$ vehicles following each other in a single lane without passing. The dynamics of each vehicle $i = 1, \ldots, N$ are governed by system (2), (3). Each vehicle can measure its own speed, the relative speed with the preceding vehicle, and the spacing with respect to the preceding vehicle. The control input (i.e., desired acceleration) of each vehicle is communicated to the following vehicle via V2V communication.

C. Predictor-Feedback CACC Design

The predictor-based control laws for system (2), (3) are given by (see [10])

$$u_i(t) = \frac{\alpha}{h} q_{i,1}(t) - (\alpha + b)\, q_{i,2}(t) + b q_{i,3}(t), \tag{5}$$

$$q_i(t) = e^{\Gamma D}\bar{x}_i(t) + \int_{t-D}^{t} e^{\Gamma(t-\theta)}\left(Bu_i(\theta) + B_1 u_{i-1}(\theta)\right) d\theta, \tag{6}$$

where

$$q_i = \begin{bmatrix} q_{i,1} \\ q_{i,2} \\ q_{i,3} \end{bmatrix}, \quad \bar{x}_i = \begin{bmatrix} s_i \\ v_i \\ v_{i-1} \end{bmatrix}, \tag{7}$$

$$B = \begin{bmatrix} 0 \\ 1 \\ 0 \end{bmatrix}, \quad B_1 = \begin{bmatrix} 0 \\ 0 \\ 1 \end{bmatrix}, \tag{8}$$

$$\Gamma = \begin{bmatrix} 0 & -1 & 1 \\ 0 & 0 & 0 \\ 0 & 0 & 0 \end{bmatrix}. \tag{9}$$

Control law (5) utilizes the D-time units ahead predictor states of $\bar{x}_i$, namely, q_i (this can be proved as in [4]). Since the nominal design (4) utilizes feedback of the preceding vehicle's speed, measurements of the control input of the preceding vehicle are required, in order to implement the predictor state for v_{i-1}. Such measurements can be obtained through V2V communication. Furthermore, control law (5) requires measurements of the ego vehicle's spacing, speed, and desired acceleration, as well as measurements of the relative speed with the preceding vehicle. All these can be obtained through on-board sensors. The only model parameter that control law (5) employs is the actuator delay D.

III. Collisions Avoidance and Non-Overshooting Response Under Predictor-Feedback CACC

Theorem 1: Consider a platoon of vehicles with dynamics modeled by (2), (3), under the control laws (5) and with the leading vehicle satisfying $v_{l0} + \int_0^t u_l(s - D)\, ds > 0$, for all $t \geq 0$.[1] There exist parameters p_1, p_2, satisfying

$$p_2 < p_1 < 0, \tag{10}$$

$$0 < -hp_1p_2 - p_1 - p_2 \leq -p_2, \tag{11}$$

such that with the choice of control gains

$$\alpha = hp_1p_2, \tag{12}$$

$$b = -hp_1p_2 - p_1 - p_2, \tag{13}$$

[1] In fact, v_l needs to be upper/lower bounded, which is the case in practice.

and for any $D \geq 0$, $h > 0$, the platoon is $\mathcal{L}_p$, $p \in [1, \infty]$, string stable and the systems' solutions satisfy

$$s_i(t) > 0, \quad v_i(t) > 0, \quad i = 1, 2, \ldots, N, \tag{14}$$

for all $t \geq 0$, provided that the initial conditions s_{i0}, v_{i0}, $v_{l0} \in \mathbb{R}$ and u_{i0},[2] $u_{l0} \in C[-D, 0]$, $i = 1, 2, \ldots, N$, satisfy

$$\frac{v_{i0} + \int_{-D}^{0} u_{i0}(s)ds}{s_{i0} + D\left(v_{i-10} - v_{i0}\right) + \int_{-D}^{0} s a_{i0}(s)ds} \leq -p_2, \tag{15}$$

where $a_{i0} = u_{i0} - u_{i-10}$, and for all $0 \leq t \leq D$

$$v_{i0} + \int_{-D}^{t-D} u_{i0}(s)ds > 0, \tag{16}$$

$$s_{i0} + t\left(v_{i-10} - v_{i0}\right) + \int_{-D}^{t-D} (D + s - t)\left(u_{i0}(s) - u_{i-10}(s)\right)ds > 0. \tag{17}$$

Furthermore, for a constant leading vehicle's speed, each individual vehicular system is asymptotically stable and zero, steady-state, spacing and speed tracking errors are achieved.

Proof: The proof can be found in Appendix A. ■

One should notice that the delay value in Theorem 1 is not restricted,[3] for a given, desired headway h. However, the control gains α, b have to be properly restricted. (Note that the placement of poles p_1 and p_2 on the real axis, which can be guaranteed by design, is necessary for guaranteeing string stability in $\mathcal{L}_\infty$, and thus, non-overshooting response, as well as for guaranteeing non-negative impulse response, which is also desirable as it implies non-oscillatory response.) Furthermore, certain (sufficient only) restrictions on initial conditions have to be satisfied. Conditions (15) imply that positivity of speed and spacing (and thus, also collision avoidance) are guaranteed when the spacing of the ego vehicle, at the time at which the platoon starts operating in closed loop (i.e., at $t = D$), is sufficiently large, in relation to its respective speed, which is reasonably expected form a viewpoint of collision avoidance. This condition guarantees positivity of spacing and speed states after the dead-time interval. For the time interval during the dead time, where each vehicle operates in open loop, positivity of states is guaranteed by conditions (16), (17), which do not involve any control parameters, as expected (in particular, for $t = 0$ they reduce to $s_{i0} > 0$ and $v_{i0} > 0$). In the specific case where the initial conditions for vehicles' accelerations are identically equal to zero, collisions are avoided, during the dead time, provided that the initial spacing s_{i0} is larger than the space reduction, between an ego vehicle and its preceding vehicle, which occurs within D time units and for constant speeds, i.e., larger than $D\left(v_{i0} - v_{i-10}\right)$. In particular, if the initial speed of the preceding vehicle is larger, collision is avoided for any positive initial spacing of the ego vehicle.

Note also that properly restricting the initial conditions is necessary for a CTH-based predictor-feedback CACC policy to guarantee positivity of states. The reason is that the nominal CTH policy, in the delay-free case, cannot guarantee positivity of states for any positive initial condition, which can be shown using, for example, Theorem 2 in [12] and the specific form of the respective closed-loop systems (which is the same with the case $D > 0$, for $t \geq D$, under predictor feedback). Thus, the conditions on control parameters are imposed both to guarantee positivity of states and string stability. In particular, under restrictions (15)–(17) on initial conditions, the sufficient conditions guaranteeing non-negative impulse response (with respect to preceding vehicle's speed variations), and thus, also $\mathcal{L}_\infty$ string stability (namely, (10), (11); see Appendix A), are also sufficient for guaranteeing positivity of spacing and speed states. Conditions (10), (11) are satisfied when either $p_2 \leq -\frac{1}{h} < p_1 < 0$ or $-\frac{2}{h} < p_1 < -\frac{1}{h}$ and $-\frac{p_1}{1+hp_1} < p_2 < p_1$.

Example 1: We illustrate here conditions (15)–(17) with respect to various delay values. We consider a case in which $p_1 = -\frac{1}{2h}$, $p_2 = -\frac{2}{h}$, while $v_{i0} = 2v_{l0} > 0$, $i = 1, \ldots, N$ and (for simplicity) $u_{i0} \equiv 0$, $i = 0, 1, \ldots, N$ (i.e., the initial conditions for commanded accelerations are identically equal to zero). In such a case, conditions (15)–(17) reduce to

$$s_{i0} \geq \frac{h}{2} v_{i0}, \quad i = 2, \ldots, N, \tag{18}$$

$$s_{10} \geq v_{10} \frac{D + h}{2}. \tag{19}$$

Since for $i = 2, \ldots, N$ the initial conditions for speeds are identical, the respective spacings do not reduce during the dead-time interval (for zero accelerations), and thus, the condition for collisions avoidance is independent of the delay value. For $i = 1$, the initial spacing has to be sufficiently large, also depending on the delay size, as during the dead-time interval the respective spacing is reduced. Thus, depending on the delay size, the initial spacing may be restricted to be larger than the desired equilibrium spacing (i.e., hv_1). This is the case when $D > h$ as for s_1 to remain positive both during the dead-time interval (where feedback control has no effect) and after control "kicks in" (resulting in certain transients), the initial spacing has to be larger than h. Vice versa, if the initial spacing is not restricted, then the delay size has to be limited. For example, if initial spacings are at equilibrium, i.e., $s_{i0} = hv_{i0}$, $i = 1, \ldots, N$, then it follows that for (19) to hold, it should be the case that $D \leq h$. We show in Fig. 2 the regions of allowable initial conditions in the (s_{10}, v_{10}) plane. There is a trade-off between the size of the set of allowable initial conditions and the size of delay.

IV. String Stability Robustness of Predictor-Feedback CACC to Delay Mismatch

Since the only parameter employed for control implementation in (5) is the delay D, we study here string stability under uncertainty in the knowledge of its value. We define as D_{r} the real delay value, and thus, we write (3) as

$$\dot{v}_i(t) = u_i\left(t - D_{\mathrm{r}}\right), \quad i = 0, 1, \ldots N. \tag{20}$$

Theorem 2: Consider a homogeneous platoon of vehicles with dynamics modeled by (2), (20), under the control laws (5). If $\alpha + 2b - \frac{2}{h} > 0$, there exists a positive constant ϵ such

[2]In fact, $u_{i0} \in C[-D, 0]$ being compatible with the feedback laws (5).

[3]Nevertheless, one could indeed restrict D for allowing larger initial conditions deviations (see also Example 1 and Fig. 2).

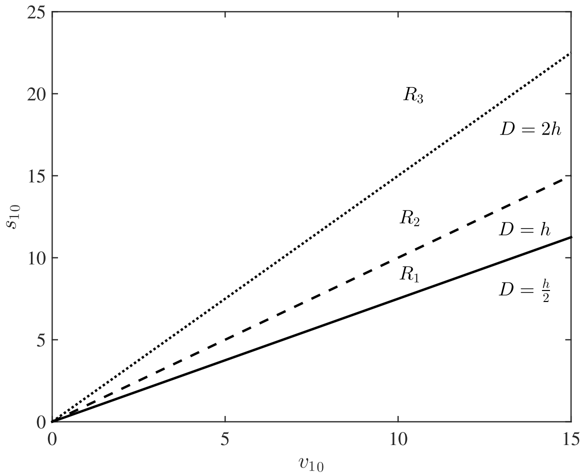

Fig. 2. Regions of allowable initial conditions (s_{10}, v_{10}), to guarantee positivity of spacings and speeds in Example 1, as the delay value varies. As delay value D increases the allowable region shrinks. In particular, from the set $R_1 \cup R_2 \cup R_3 = \left\{s_{10} > 0, v_{10} > 0 : s_{10} \geq v_{10}\frac{3h}{4}\right\}$ for $D = \frac{h}{2}$ to $R_3 = \left\{s_{10} > 0, v_{10} > 0 : s_{10} \geq v_{10}\frac{3h}{2}\right\}$ for $D = 2h$.

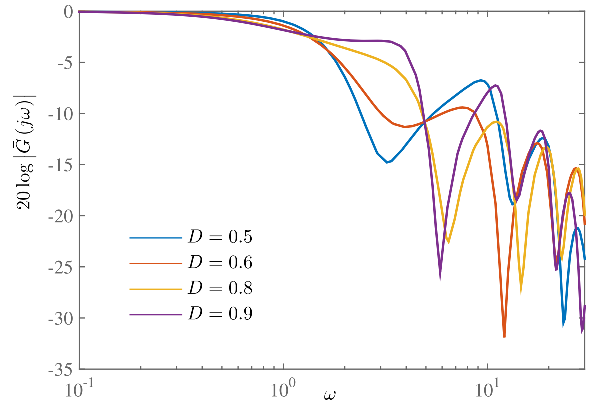

Fig. 3. Bode diagram of the magnitude of the transfer function (B.11) for four different values of the delay D that is available to the designer, namely $D \in \{0.5, 0.6, 0.8, 0.9\}$. The real value of the delay is $D_{\rm r} = 0.7$.

that for all $|\Delta D| = |D_{\rm r} - D| < \epsilon$ and any D, $D_{\rm r} \geq 0$, $h > 0$, the platoon is $\mathcal{L}_2$ string stable. Furthermore, for a constant leading vehicle's speed, each individual vehicular system is asymptotically stable and zero, steady-state, spacing and speed tracking errors are achieved.

Proof: The proof can be found in Appendix B. ∎

In the case in which there is delay mismatch in the actual delay $D_{\rm r}$ and the delay D available to the designer, this mismatch should be sufficiently small (to guarantee that stability and $\mathcal{L}_2$ string stability are preserved), and thus, the designer should be able to choose a delay value that is close enough to the actual delay value. However, the delay values themselves, i.e., both the delay available to the designer D and the actual delay $D_{\rm r}$ are not restricted (only $|D - D_{\rm r}|$ is restricted).

Example 2: We illustrate $\mathcal{L}_2$ string stability robustness to delay mismatch through an example with $D_{\rm r} = 0.7$, $p_1 = -0.1$, $p_2 = -1.5$, and $h = 0.75$ (that also satisfy conditions (10), (11)).[4] In Fig. 3 we show $\left|\bar{G}(j\omega)\right|$ defined in (B.11) for four different values of the delay D that is available to the designer. We observe that $\left|\bar{G}(j\omega)\right|$ never exceeds unity for all $D \in [0.5, 0.9]$ (it is verified in simulation that asymptotic stability is also preserved within this range for D).

V. Simulation Results

We illustrate here the safety properties of CTH-based predictor-feedback CACC with a platoon of five vehicles. We consider first a case in which $D_{\rm r} = D = 0.7$, $h = 0.75$ and choose $p_1 = -0.1$, $p_2 = -1.5$, which satisfy conditions (10), (11). We consider a scenario in which $u_{i0} \equiv 0$, for $i = 0, 1, \ldots, N$, and $s_{i0} = hv_{i0} = 0.75 \times 15$ m, $i = 2, 3, 4$, while we set $v_{10} = \frac{2v_{10}}{3} = 10 \left(\frac{\rm m}{\rm s}\right)$ and $s_{10} = 13.55$ m. This scenario could correspond to a vehicle cutting-in into a platoon of four vehicles. After the effect of initial conditions has faded away, in the scenario considered, the leading vehicle performs a (strong) decelerating and then an accelerating maneuver. Thus, this scenario illustrates the effectiveness of the proposed design with respect to both initial conditions deviations from equilibrium and leading vehicle's maneuvers. As it is shown in Fig. 4, positivity of speed and spacing states is achieved, while the responses to the leading vehicle's maneuvers feature no oscillation and no overshoot, as result of the achieved impulse response positivity and $\mathcal{L}_\infty$ string stability, respectively.

In the scenario considered, since initial conditions for accelerations are zero and since initial conditions for speeds for vehicles indexed with $i = 2, 3, 4$ are equal to each other (and positive), conditions (15)–(17) reduce to $v_{i0} \leq -p_2 s_{i0}$, for $i = 2, 3, 4$ and $v_{10} \leq -p_2\left(s_{10} - \frac{D}{3}v_{10}\right)$. Thus, for the choice $s_{i0} = hv_{i0}$, for $i = 2, 3, 4$ the former conditions hold given that $p_2 \leq -\frac{1}{h}$, while the latter holds provided that $s_{10} \geq v_{10}\left(-\frac{1}{p_2} + \frac{D}{3}\right)$, which is satisfied in the present scenario. This condition expresses the fact that, for collisions to be avoided, initial spacing between the first vehicle in platoon and the vehicle cutting-in is sufficiently large, depending proportionally on the delay size and respective, initial speed.

In Fig. 5 we show the response of the platoon for uncertain delay. We consider initial conditions at an equilibrium dictated by a constant leader's speed, namely, $u_{i0}(s) = 0$, $-D \leq s < 0$, $v_{i0} = 10 \left(\frac{\rm m}{\rm s}\right)$, $i = 0, \ldots, 4$, and $s_{i0} = hv_{i0}$, $i = 1, 2, 3, 4$. For such a scenario conditions (15)–(17) reduce to $p_2 \leq -\frac{1}{h}$, which is satisfied (as (11) holds). The leading vehicle performs an acceleration/deceleration maneuver. Although respective responses exhibit oscillations and overshoot, $\mathcal{L}_2$ string stability is preserved. This is illustrated in Fig. 6 that shows functions $\|\delta_i\|_{2,t} = \sqrt{\int_0^t \delta_i(s)^2 ds}$. Relations $\|\delta_i\|_{2,t} \leq \|\delta_{i-1}\|_{2,t}$, $i = 2, 3, 4$, hold for all $t \geq 0$ (and thus, so do (1) for $p = 2$). The responses to leading vehicle's maneuvers are dictated by transfer function (B.11), which, in contrast to the uncertainty-free case (A.19), it involves delay terms in both

[4] Note that when all initial states are at an equilibrium, dictated by a constant, positive speed v^* of the leader, i.e., $u_{i0} \equiv 0$, $v_{i0} = v^*$, for $i = 0, 1, \ldots, N$, and $s_{i0} = hv_{i0}$, $i = 1, \ldots, N$, conditions (15)–(17) hold provided that $p_2 \leq -\frac{1}{h}$. The latter condition is anyway imposed by condition (11) as a requirement for non-negative impulse response (and thus, for $\mathcal{L}_\infty$ string stability; see also Appendix A for details). The fact that, in this case, the conditions required for achieving (14) reduce to delay-free conditions, is a result of predictor-feedback achieving delay compensation after D time units.

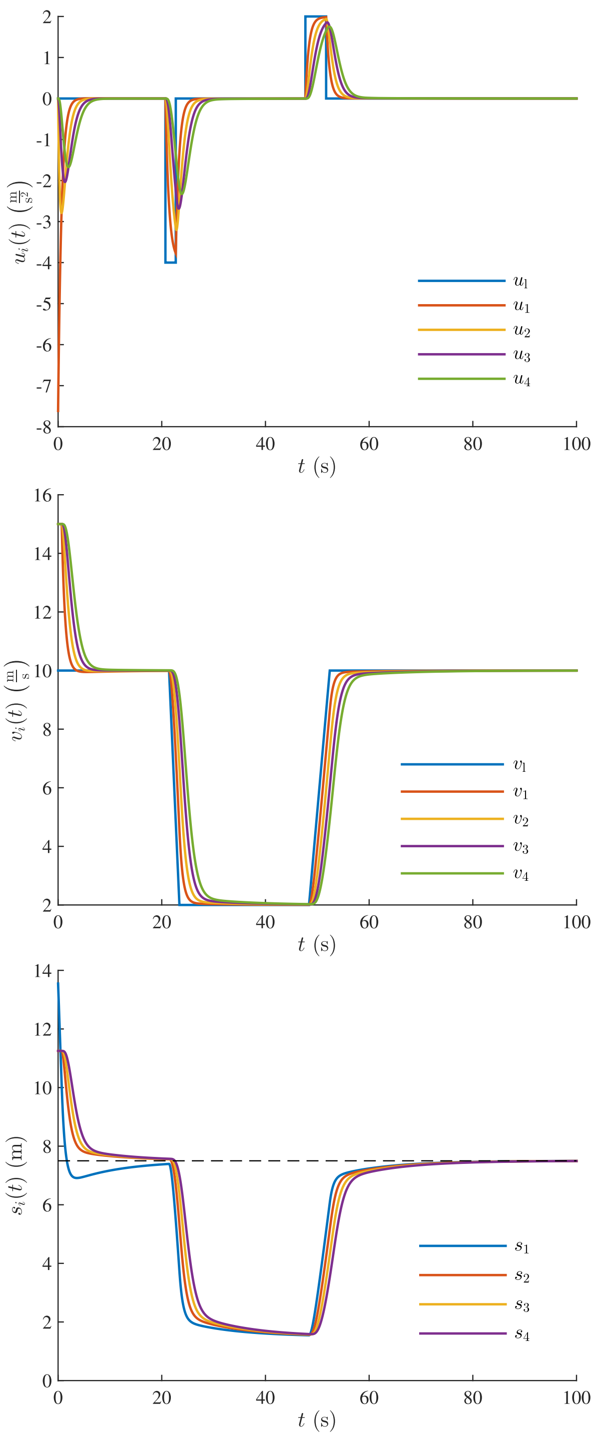

Fig. 4. Commanded acceleration (top), speed (middle), and spacing (bottom) of four vehicles following a leader that performs an acceleration/deceleration maneuver, under the CTH predictor-feedback CACC law (5). Initial conditions are $s_{1\,0} = 13.55$ m, $s_{i\,0} = hv_{i\,0} = 0.75 \times 15$ m, $i = 2, 3, 4$, $v_{l\,0} = 10$, $v_{i\,0} = 15$ $\left(\frac{\mathrm{m}}{\mathrm{s}}\right)$, $i = 1, 2, 3, 4$, $u_{i\,0}(s) = 0$, $-D \leq s < 0$, for $i = 0, \dots, 4$.

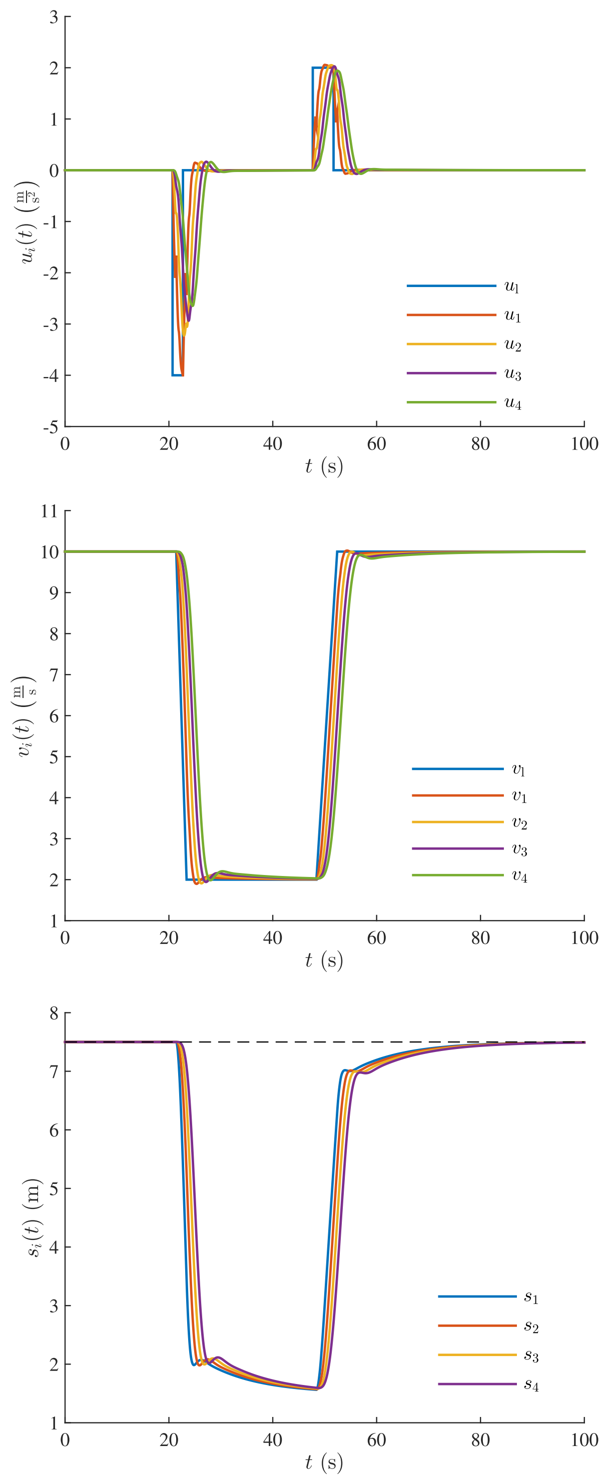

Fig. 5. Commanded acceleration (top), speed (middle), and spacing (bottom) of four vehicles following a leader that performs an acceleration/deceleration maneuver, under the CTH predictor-feedback CACC strategy (5). Initial conditions are at equilibrium. The actual value of the delay is $D_{\mathrm{r}} = 0.7$, while the delay value available to the designer is $D = 0.5$.

the numerator and the denominator. Therefore, although all poles are on the left half of the complex plane, the delay terms appearing in numerator/denominator result in a response that features oscillations. In particular, this is attributed to appearance of complex roots in the denominator (that could be shown, for example, numerically computing the respective roots).

VI. Extension to Heterogeneous Vehicles With Third-Order Dynamics

The extension to heterogeneous, third-order dynamics and nominal control parameters (i.e., desired headways and control gains) is conceptually straightforward, however, it is computationally (and notationally) cumbersome. Because the main

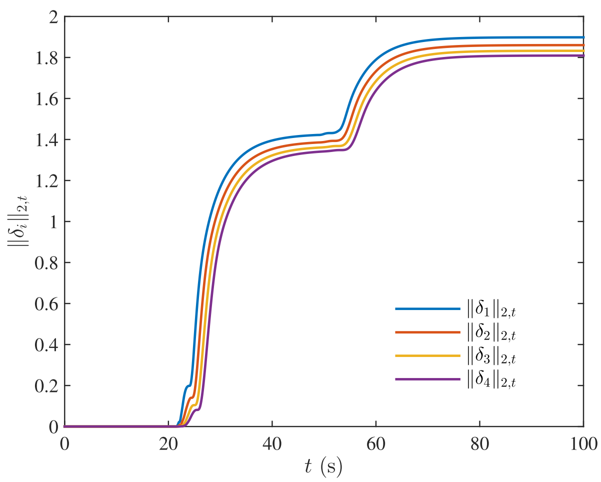

Fig. 6. Norms $\|\delta_i\|_{2,t} = \sqrt{\int_0^t \delta_i(s)^2 ds}$ corresponding to Fig. 5's scenario.

scope of the paper is to illustrate the safety, string stability, and delay-robustness properties of predictor-feedback CACC, we focus on the computationally and notationally simpler second-order dynamics in order to more clearly illustrate the main design and analysis ideas without distracting the reader with tedious algebraic computations. Nevertheless, for the reader's benefit, we demonstrate in this section such an extension, presenting the predictor-feedback CACC design, elements from the respective analysis, and consistent simulation results.

The second-order model with input delay still provides some insight and it could be used for assessing the benefits of the delay-compensating mechanism to traffic flow (and not necessarily to the performance of each individual vehicle), through analyzing stability, string stability, and safety of CAVs platoons. Such second-order car-following-type models are actually utilized in literature to analyze the effects on traffic flow of ACC/CACC designs, through analyzing safety and string stability with and without delays, see, for example, [13], [14], [15], [25], [38], and [39] and [2], [3], [8], and [20], respectively. In fact, although a second-order model may not capture underlying, low level engine (and other powertrain) dynamics, the benefits of the delay-compensating mechanism of the presented predictor-feedback CACC design to stability, string stability, and safety are indeed illustrated, since such a feedback law could be viewed, in practice, as implemented within an outer control loop (in a complete feedback loop accounting for lower level vehicle dynamics), with an inner control loop addressing powertrain dynamics (see, e.g., [29]).

A. Predictor-Feedback CACC Design

We consider the following system for $i = 1, \ldots, N$

$$\dot{s}_i(t) = v_{i-1}(t) - v_i(t), \tag{21}$$
$$\dot{v}_i(t) = a_i(t), \tag{22}$$
$$\dot{a}_i(t) = -\frac{1}{\tau_i} a_i(t) + \frac{1}{\tau_i} u_i(t-D), \tag{23}$$

where a_i is vehicle acceleration and τ_i is lag, capturing, for example, engine dynamics (with $\dot{v}_1(t) = a_1(t)$, $\dot{a}_1(t) = -\frac{1}{\tau_1} a_1(t) + \frac{1}{\tau_1} u_1(t-D)$). For designing a delay-compensating predictor-feedback law we modify the nominal law (4) to

$$u_i(t) = \tau_i \alpha_i \left(\frac{s_i(t)}{h_i} - v_i(t) \right) + \tau_i b_i \left(v_{i-1}(t) - v_i(t) \right) + \tau_i c_i a_i(t), \tag{24}$$

with the choice

$$\alpha_i = -h_i p_i^3, \tag{25}$$
$$b_i = h_i p_i^3 + 3p_i^2, \tag{26}$$
$$c_i = \frac{1}{\tau_i} + 3p_i, \tag{27}$$

for some $p_i < 0$. For simplicity of presentation (even though we sacrifice design flexibility), as our aim in this section is to illustrate that such an extension is possible, we choose, for each vehicular system, the closed-loop poles of the nominal, delay-free case identical and equal to p_i. Note that a predictor-feedback CACC design could be constructed with other choices for the nominal ACC (or CACC) law. For the same reason we choose a simple modification of (4), to mainly illustrate that it is conceptually straightforward to incorporate third-order dynamics and heterogeneity in h and τ. The predictor-feedback CACC law becomes

$$u_i(t) = \frac{\tau_i \alpha_i}{h_i} q_{i,1}(t) - \tau_i (\alpha_i + b_i) q_{i,2}(t) + \tau_i b_i q_{i,3}(t) + \tau_i c_i q_{i,4}(t), \tag{28}$$
$$q_i(t) = e^{\Gamma_i D} \bar{x}_i(t) + \int_{t-D}^{t} e^{\Gamma_i (t-\theta)} \left(B_i u_i(\theta) + B_{1_i} u_{i-1}(\theta) \right) d\theta, \tag{29}$$

where

$$q_i = \begin{bmatrix} q_{i,1} \\ q_{i,2} \\ q_{i,3} \\ q_{i,4} \\ q_{i,5} \end{bmatrix}, \quad \bar{x}_i = \begin{bmatrix} s_i \\ v_i \\ v_{i-1} \\ a_i \\ a_{i-1} \end{bmatrix}, \tag{30}$$

$$B_i = \begin{bmatrix} 0 \\ 0 \\ 0 \\ \frac{1}{\tau_i} \\ 0 \end{bmatrix}, \quad B_{1_i} = \begin{bmatrix} 0 \\ 0 \\ 0 \\ 0 \\ \frac{1}{\tau_{i-1}} \end{bmatrix}, \tag{31}$$

$$\Gamma_i = \begin{bmatrix} 0 & -1 & 1 & 0 & 0 \\ 0 & 0 & 0 & 1 & 0 \\ 0 & 0 & 0 & 0 & 1 \\ 0 & 0 & 0 & -\frac{1}{\tau_i} & 0 \\ 0 & 0 & 0 & 0 & -\frac{1}{\tau_{i-1}} \end{bmatrix}. \tag{32}$$

Note that, due to employment of a third-order dynamical model, in order to design the predictor state for v_i and v_{i-1} we should also incorporate the dynamics of a_i and a_{i-1}, respectively, which increase the order of q_i. All required measurements for control implementation can be obtained via onboard sensors or V2V communication.

B. Positivity of Spacing and Speed States

Using the delay-compensating property of predictor feedback and (25)–(27), proceeding in a similar manner to the proof of Theorem 1, we have for $t \geq D$ that

$$\begin{bmatrix} \dot{s}_i(t) \\ \dot{v}_i(t) \\ \dot{a}_i(t) \end{bmatrix} = \begin{bmatrix} 0 & -1 & 0 \\ 0 & 0 & 1 \\ -p_i^3 & -3p_i^2 & 3p_i \end{bmatrix} \times \begin{bmatrix} s_i(t) \\ v_i(t) \\ a_i(t) \end{bmatrix} + \begin{bmatrix} 1 \\ 0 \\ b_i \end{bmatrix} v_{i-1}(t). \quad (33)$$

The solution to (33) is given as

$$\begin{bmatrix} s_i(t) \\ v_i(t) \\ a_i(t) \end{bmatrix} = \mathrm{e}^{\bar{A}_i(t-D)} \begin{bmatrix} s_i(D) \\ v_i(D) \\ a_i(D) \end{bmatrix} + \int_D^t \mathrm{e}^{\bar{A}_i(t-s)} \begin{bmatrix} 1 \\ 0 \\ b_i \end{bmatrix} v_{i-1}(s)ds, \quad (34)$$

where

$$\bar{A}_i = \begin{bmatrix} 0 & -1 & 0 \\ 0 & 0 & 1 \\ -p_i^3 & -3p_i^2 & 3p_i \end{bmatrix}.$$

Computing explicitly the first two rows of $\mathrm{e}^{\bar{A}_i t}$ we obtain with $t^* = t - D$

$$s_i(t) = \mathrm{e}^{p_i(t-D)}\left(s_i(D)\frac{(p_i t^* - 1)^2 + 1}{2} + t^* v_i(D) \times \left(t^* p_i - 1\right) - a_i(D)\frac{t^{*2}}{2}\right) + \int_D^t \mathrm{e}^{p_i(t-s)} v_{i-1}(s) \times \left(\frac{(p_i(t-s) - 1)^2 + 1}{2} - b_i \frac{(t-s)^2}{2}\right) ds, \quad (35)$$

$$v_i(t) = \mathrm{e}^{p_i(t-D)}\left(-\frac{t^{*2} p_i^3}{2} s_i(D) - v_i(D)\left(t^{*2} p_i^2 + t^* p_i - 1\right) + a_i(D)\frac{t^*(p_i t^* + 2)}{2}\right) + \int_D^t \mathrm{e}^{p_i(t-s)} v_{i-1}(s) \times \left(-\frac{p_i^3 (t-s)^2}{2} + \frac{b_i(t-s)(p_i(t-s)+2)}{2}\right) ds. \quad (36)$$

From (35), (36), imposing the condition $0 \leq b_i \leq p_i^2$, which, using (26), is satisfied provided that for all $i = 1, \ldots, N$ it holds that $-\frac{3}{h_i} \leq p_i \leq -\frac{2}{h_i}$, as well as the following conditions

$$s_i(D) > \frac{1}{-p_i}\left(2v_i(D) + \frac{a_i(D)}{-p_i}\right), \quad (37)$$

$$v_i(D) > \max\left\{\frac{a_i(D)}{p_i}, 0\right\}, \quad (38)$$

we guarantee by induction (similarly to the proof of Theorem 1) that $s_i(t) > 0$, $v_i(t) > 0$, $i = 1, \ldots, N$, for all $t \geq D$ (under the assumption that $v_1(t) > 0$ for all $t \geq 0$). As in the proof of Theorem 1 to guarantee that (37), (38) hold we need to impose certain conditions on the initial conditions. This is a fundamental limitation as during the dead-time interval each feedback law does not affect the respective vehicle. During the dead-time interval we have from (22), (23) that

$$\begin{bmatrix} \dot{v}_i(t) \\ \dot{a}_i(t) \end{bmatrix} = \begin{bmatrix} 0 & 1 \\ 0 & -\frac{1}{\tau_i} \end{bmatrix} \begin{bmatrix} v_i(t) \\ a_i(t) \end{bmatrix} + \begin{bmatrix} 0 \\ \frac{1}{\tau_i} \end{bmatrix} u_{i_0}(t-D), \quad (39)$$

and thus, solving (39) for v_i, it follows that to guarantee positivity of speed for $0 \leq t \leq D$ it should hold that

$$v_i(0) + \tau_i\left(1 - \mathrm{e}^{-\frac{t}{\tau_i}}\right) a_i(0) + \int_0^t \left(1 - \mathrm{e}^{-\frac{t-s}{\tau_i}}\right) u_{i_0}(s-D)ds > 0, \quad \forall\, 0 \leq t \leq D. \quad (40)$$

Therefore, solving (21) for $s_i(t)$ we obtain that to guarantee that $s_i(t) > 0$ for $0 \leq t \leq D$ it should hold that

$$s_i(0) + t\left(v_{i-1}(0) - v_i(0)\right) + \tau_{i-1}a_{i-1}(0) \times \left(t + \tau_{i-1}\mathrm{e}^{-\frac{t}{\tau_{i-1}}} - \tau_{i-1}\right) - \tau_i a_i(0) \times \left(t + \tau_i \mathrm{e}^{-\frac{t}{\tau_i}} - \tau_i\right) + \int_0^t (t - s + \tau_{i-1} \times \left(\mathrm{e}^{-\frac{t-s}{\tau_{i-1}}} - 1\right)\Big) u_{i-1_0}(s-D)ds - \int_0^t \left(t - s + \tau_i\left(\mathrm{e}^{-\frac{t-s}{\tau_i}} - 1\right)\right) \times u_{i_0}(s-D)ds > 0, \quad \forall\, 0 \leq t \leq D. \quad (41)$$

Furthermore, to satisfy conditions (37), (38), we use the left-hand sides of (40) and (41) for $t = D$ (that define $v_i(D)$ and $s_i(D)$, respectively), as well as the following relation, which defines $a_i(t)$ for $0 \leq t \leq D$

$$a_i(t) = \mathrm{e}^{-\frac{t}{\tau_i}} a_i(0) + \int_0^t \mathrm{e}^{-\frac{t-s}{\tau_i}} u_{i_0}(s-D)ds, \ 0 \leq t \leq D. \quad (42)$$

To more clearly illustrate conditions (37), (38) we consider a case with zero initial conditions for accelerations and control inputs, i.e., $a_{i_0} = 0$ and $u_{i_0} \equiv 0$, $i = 0, 1, \ldots, N$. In such a case, conditions (37), (38), using (40)–(42), are written as

$$v_{i_0} > 0, \quad (43)$$

$$s_{i_0} > D\left(v_{i_0} - v_{i-1_0}\right) + \frac{2v_{i_0}}{-p_i}. \quad (44)$$

Conditions (43), (44) are realistic from a practical viewpoint. In particular, condition (44) requires the initial spacing to be sufficiently large, both depending on its initial speed difference with respect to the preceding vehicle; as during the dead-time interval the control input cannot affect the ego vehicle, as well as depending on the initial speed of the ego vehicle; since after control "kicks in" at time $t = D$ the transients of s_i should be such that positivity is guaranteed, which requires the right-hand side of (44) to depend also on its second term (see also the discussion immediately after the statement of Theorem 1).

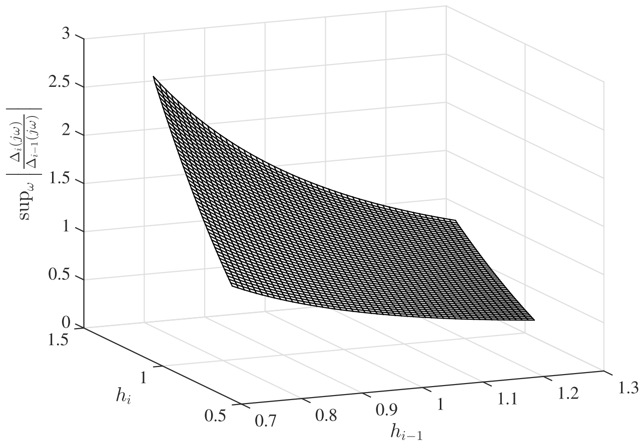

Fig. 7. The values $\sup_\omega \left|\frac{\Delta_i(j\omega)}{\Delta_{i-1}(j\omega)}\right|$ corresponding to (48) for fixed $\lambda_i = 2.5$ and variable $0.75 \le h_i \le 1.25$, $0.75 \le h_{i-1} \le 1.25$.

C. Stability and String Stability

To analyze the stability and string stability properties of the closed-loop system we proceed as in the proof of Theorem 1. Asymptotic stability and zero steady-state tracking error follow from (33). The transfer function $G_i = \frac{V_i}{V_{i-1}}$ corresponding to the closed-loop system (21)–(23), (28)–(32), with (25)–(27), is computed in a similar manner to the proof of Theorem 1 as

$$G_i(s) = \frac{V_i(s)}{V_{i-1}(s)} = \frac{-p_i^3 + p_i^2\,(p_i h_i + 3)\,s}{(s - p_i)^3}. \tag{45}$$

String stability in $\mathcal{L}_p$, $p \in [1, +\infty]$, since $G_i(0) = 1$, follows whenever (45) corresponds to a non-negative impulse response (see, e.g., [7]). From [23] (Theorem 5; case Type D-1)), the latter holds true when the following condition holds

$$-\frac{1}{p_i} \ge -\frac{h_i}{p_i}\left(p_i + \frac{3}{h_i}\right) \ge 0, \tag{46}$$

which is satisfied provided that $-\frac{3}{h_i} \le p_i \le -\frac{2}{h_i}$. In a similar manner we can obtain the spacing error transfer functions as

$$\frac{\Delta_i(s)}{\Delta_{i-1}(s)} = \frac{p_{i-1}^2(s\,(3 + h_{i-1}p_{i-1}) - p_{i-1})(s - z_i)}{(s - p_i)^3(s - \bar{p}_{i-1})}, \tag{47}$$

where $z_i = p_i^3 h_i^2 + 3p_i^2 h_i + 3p_i$ and $\bar{p}_{i-1} = h_{i-1}^2 p_{i-1}^3 + 3h_{i-1}p_{i-1}^2 + 3p_{i-1}$. To evaluate $\mathcal{L}_2$ string stability (note that $\bar{p}_{i-1} = p_{i-1}\left(\left(h_{i-1}p_{i-1} + \frac{3}{2}\right)^2 + \frac{3}{4}\right) < 0$) we choose $p_i = -\frac{\lambda_i}{h_i}$ for some $2 \le \lambda_i \le 3$ and for all $i = 1, \ldots, N$ to obtain

$$\frac{\Delta_i(s)}{\Delta_{i-1}(s)} = \frac{\frac{\lambda_{i-1}^2}{h_{i-1}^2}\left(s(3 - \lambda_{i-1}) + \frac{\lambda_{i-1}}{h_{i-1}}\right)(s - z_i)}{\left(s + \frac{\lambda_i}{h_i}\right)^3 (s - \bar{p}_{i-1})}, \tag{48}$$

$z_i = -\frac{\lambda_i}{h_i}\left(\lambda_i^2 + 3\lambda_i + 3\right)$, $\bar{p}_{i-1} = -\frac{\lambda_{i-1}}{h_{i-1}}\left(\lambda_{i-1}^2 + 3\lambda_{i-1} + 3\right)$. We show in Fig. 7 the values of $\sup_\omega \left|\frac{\Delta_i(j\omega)}{\Delta_{i-1}(j\omega)}\right|$ for fixed $\lambda_i = 2.5$ and variable $0.75 \le h_i \le 1.25$ and $0.75 \le h_{i-1} \le 1.25$. String stability is preserved within the range of (h_i, h_{i-1}) such that $\sup_\omega \left|\frac{\Delta_i(j\omega)}{\Delta_{i-1}(j\omega)}\right| \le 1$. In fact, it should necessarily hold that $\left|\frac{\Delta_i(0)}{\Delta_{i-1}(0)}\right| = \frac{h_i^2}{h_{i-1}^2} \le 1$, $i = 2, \ldots, N$. Thus, as the latter condition may be restrictive (although feasible), for string stability with respect to spacing errors, one could either adopt a different definition, such as, e.g., head-to-tail

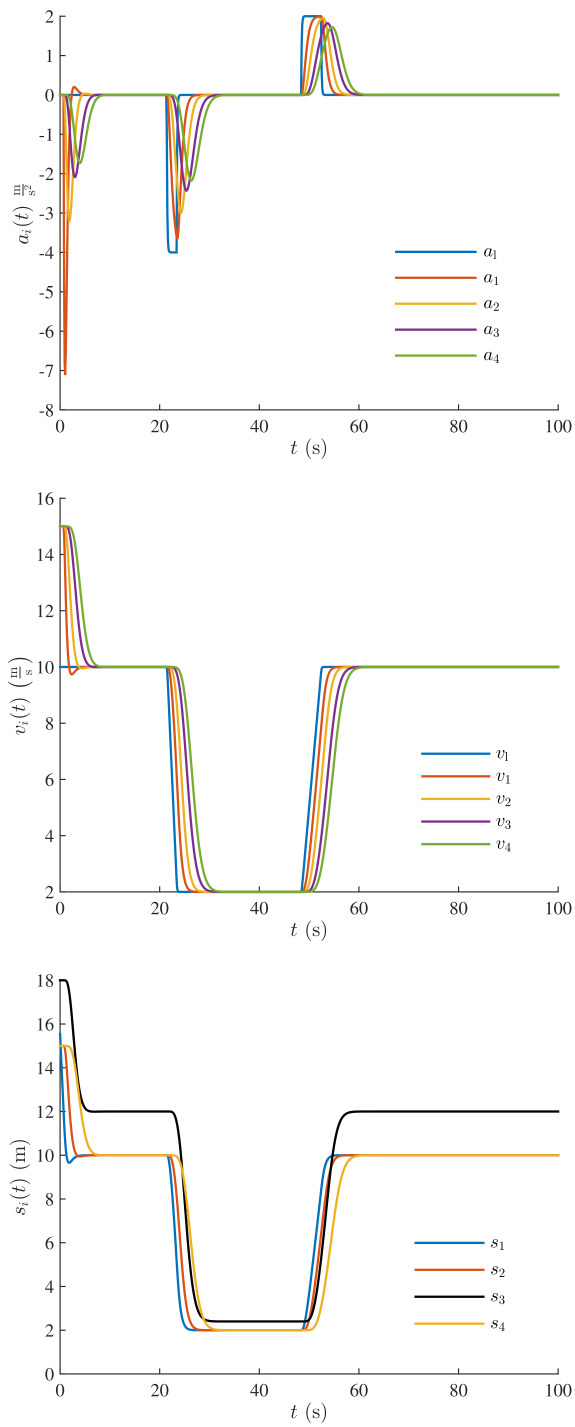

Fig. 8. Acceleration (top), speed (middle), and spacing (bottom) of four vehicles, with dynamics given by (21)–(23), following a leader that performs an acceleration/deceleration maneuver, under the CTH predictor-feedback CACC laws (28). Initial conditions are $s_{1_0} = 15.55$ m, $s_{i_0} = h_i v_{i_0} = h_i \times 15$ m, $i = 2, 3, 4$, $v_{l_0} = 10$, $v_{i_0} = 15\ \left(\frac{m}{s}\right)$, $i = 1, 2, 3, 4$, and $a_{i_0} = 0$, $u_{i_0}(s) = 0$, $-D \le s < 0$, for $i = 0, \ldots, 4$. Desired headways are $h_i = 1$, $i = 1, 2, 4$ and $h_i = 1.2$, $i = 3$, while control parameters are chosen according to (25)–(27) with $p_i = -\frac{2.5}{h_i}$, $i = 1, 2, 3, 4$. Time constants τ_i for each vehicle are $\tau_i = 0.1$ s, $i = 0, 1, 2, 4$ and $\tau_i = 0.25$ s, $i = 3$.

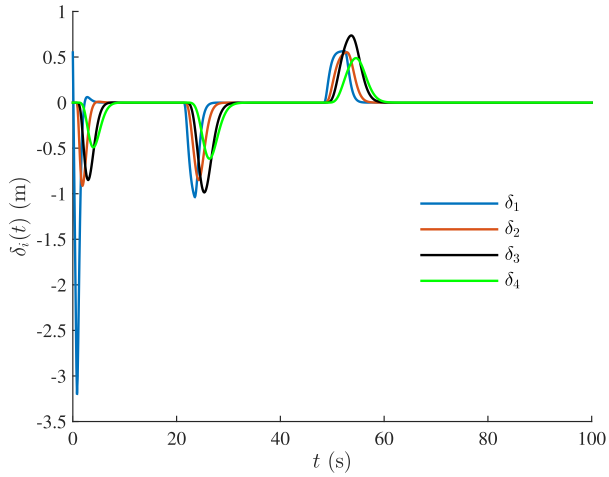

Fig. 9. Spacing errors $\delta_i(t) = s_i(t) - h_i v_i(t)$, $i = 1, 2, 3, 4$, corresponding to the responses of Fig. 8.

string stability [39] and definition $\sup_\omega \left|\frac{\Delta_i(j\omega)}{\Delta_{i-1}(j\omega)}\right| \leq \frac{h_i^2}{h_{i-1}^2}$ [35] or choose different control parameters λ_i and nominal CACC law.

D. Simulation Results

We illustrate here the performance of the CTH-based predictor-feedback CACC for a heterogeneous platoon of five vehicles with third-order dynamics given by (21)–(23). We consider a case in which $\tau_i = 0.1$, $h_i = 1$ for $i = 1, 2, 4$ and $\tau_i = 0.25$, $h_i = 1.2$ for $i = 3$ (with $\tau_1 = 0.1$). The delay is set to $D = 0.7$ and we choose the control gains according to (25)–(27) with $p_i = -\frac{2.5}{h_i}$, $i = 1, 2, 3, 4$, which satisfy condition (46). We consider a scenario in which $a_i = 0$ and $u_{i0} \equiv 0$, for $i = 0, 1, 2, 3, 4$, and $s_{i0} = h_i v_{i0} = h_i \times 15$ m, $i = 2, 3, 4$, while we set $v_{10} = \frac{2v_{10}}{3} = 10$ $\left(\frac{\text{m}}{\text{s}}\right)$ and $s_{10} = 15.55$ m, which satisfy (43), (44); while the leading vehicle performs a decelerating and then an accelerating maneuver. As it is shown in Fig. 8, positivity of speed and spacing states is achieved, while the speed and acceleration responses to the leading vehicle's maneuvers feature no oscillation and no overshoot, as result of the achieved impulse response positivity and $\mathcal{L}_\infty$ string stability, respectively; guaranteed for the respective transfer functions (45) under the condition (46). String stability with respect to spacing errors is dictated by transfer function (48). For $i = 1, 2$ string stability with respect to spacing errors follows from (45) (as in the case of speeds and accelerations), whereas for $i = 3$ and $i = 4$ it is dictated by (48) with $h_3 = 1.2$, $h_2 = 1$ and $h_4 = 1$, $h_3 = 1.2$, respectively. Thus, as it is shown in the spacing error plots in Fig. 9, spacing error perturbations are amplified as they propagate from vehicle $i = 2$ to vehicle $i = 3$ (as $\frac{h_3}{h_2} > 1$); nevertheless, they are damped as they propagate, from vehicle $i = 3$, upstream of the platoon (according to Fig. 7 since $\frac{h_4}{h_3} = \frac{1}{1.2}$).

VII. Conclusion and Future Research

In the present paper we consider the case of identical, actuator delays for all vehicles, also motivated by literature, see, for example, [10], [13], [36], and [37]. The problem of compensation of distinct actuator (and sensor) delays is a different problem than the one considered here, and thus, the presented design (and analysis) approach cannot be extended in such a case in a straightforward manner, which is explained as follows. In the case of heterogeneous (distinct) actuator delays the predictor-feedback CACC design becomes more complex and would require availability of additional measurements, stemming from V2V communication, which are not covered within the present setup, in particular, state and control input information of more than one, preceding vehicles. In fact, one would have to employ the results from [5] to the case of interconnected systems. Although (at least conceptually) this appears to be feasible, there will be certain technical challenges that would have to be overcome. In particular, in the case where the ego vehicle's actuator delay is larger than the preceding vehicle's actuator delay (i.e., $D_i > D_{i-1}$), it would not be possible to construct its predictor state directly via (6) (as this would require $u_{i-1}(\theta)$ to be replaced by $u_{i-1}(\theta + D_i - D_{i-1})$ inside the integral, which may not be available at current time). In such a case (see [5] for details), to derive the predictor state for the ego vehicle, one would have to also employ/know the feedback law of the preceding vehicle, which, eventually, would lead to a requirement that the ego vehicle has access to the states and control input of a vehicle two vehicles ahead (i.e., to the state and control input of vehicle $i-2$). This would require additional V2V communication requirements that are not addressed here (where we assume availability of minimum V2V communication requirements).

Although here we guarantee delay compensation (as well as stability and string stability) by design, positivity of speed and spacing states with respect to initial conditions deviations is essentially only analyzed (locally, i.e., established not for all positive initial conditions). Thus, as potential next step, one could combine the delay-compensating CACC mechanism presented here with nonlinear, safe ACC/CACC laws, see, e.g., [2], [3], [15], and [20], such that both elements are guaranteed in design. This may also allow to guarantee by design additional constraints in speed and acceleration states. Towards this end, one could be inspired by the results for general systems in [1], [17], and [26]. Development of nonlinear predictor-feedback CACC laws (including Lyapunov-based designs) may further enable to explicitly address (simultaneously with delay) certain nonlinear (lower level) dynamic effects, due to, e.g., hard braking and aerodynamic drag (see, e.g., [29], [42]), as well as other practical constraints, such as, e.g., input saturation.

In the present paper we do not account for communication delay, which could be also present in practice [13], [37], [40]. The reason is that, in contrast to sensing delays, which can be treated in a similar manner to actuation delays (not for analysis, but for predictor state design), one cannot directly utilize a predictor-feedback design as the current (and not the delayed) preceding vehicle's acceleration is needed in the ego vehicle's controller. In more detail, each ego vehicle employs the information of the preceding vehicle's control input over a horizon from D time-units in the past up to the current time (see the integral in (6)). Under communication delay however this information is not available (i.e., $u_{i-1}(s)$, $s \in [t-D, t]$ is not available, but rather, only $u_{i-1}(s)$, $s \in [t-D, t-t_{c_{i-1}}]$ is available, where $t_{c_{i-1}}$ is communication delay). Thus, since (at least under the present measurement requirements, vehicles' model, and employed baseline controller) it does not seem straightforward to design a predictor-feedback CACC law under communication delay, this will be addressed in future research. Towards this end, as first step, one could study robustness, of both individual vehicles stability and string stability, to small communication delay, of CTH predictor-feedback CACC, utilizing the results in [4], [19], and [21] and the proof strategy of Theorem 2.

Appendix A

Proof of Theorem 1: The signal q_i in (6) satisfies $q_i(t) = \bar{x}_i(t+D)$ for all $t \geq 0$, see, e.g., [4].[5] Therefore, under (5), for $t \geq D$ it holds that

$$\begin{bmatrix} \dot{s}_i(t) \\ \dot{v}_i(t) \end{bmatrix} = \begin{bmatrix} 0 & -1 \\ \frac{\alpha}{h} & -(\alpha+b) \end{bmatrix} \begin{bmatrix} s_i(t) \\ v_i(t) \end{bmatrix} + \begin{bmatrix} 1 \\ b \end{bmatrix} v_{i-1}(t). \tag{A.1}$$

Choosing α and b, according to (12) and (13), respectively, for some $0 > p_1 > p_2$, we place the eigenvalues of the closed-loop systems (A.1), $i = 1, 2, \ldots,$ at p_1, p_2. Thus, solving for s_i, v_i, treating v_{i-1} as exogenous input, we get for $t \geq D$ that

$$s_i(t) = \frac{1}{p_1 - p_2}\Big(-e^{p_1(t-D)}(v_i(D) + p_2 s_i(D)) + e^{p_2(t-D)}(v_i(D) + p_1 s_i(D))\Big) + r_{1,i}(t), \tag{A.2}$$

$$v_i(t) = \frac{1}{p_1 - p_2}\Big(p_1 e^{p_1(t-D)}(v_i(D) + p_2 s_i(D)) - p_2 e^{p_2(t-D)}(v_i(D) + p_1 s_i(D))\Big) + r_{2,i}(t), \tag{A.3}$$

where

$$r_{1,i}(t) = -\frac{1}{p_1 - p_2}\int_D^t \Big(e^{p_1(t-s)}(b + p_2) - e^{p_2(t-s)}(b + p_1)\Big) v_{i-1}(s)ds, \tag{A.4}$$

$$r_{2,i}(t) = \frac{1}{p_1 - p_2}\int_D^t \Big(p_1 e^{p_1(t-s)}(b + p_2) - p_2 e^{p_2(t-s)}(b + p_1)\Big) v_{i-1}(s)ds. \tag{A.5}$$

We next establish positivity of (A.2)–(A.5) under (10), (11), and condition

$$0 < v_i(D) \leq -p_2 s_i(D). \tag{A.6}$$

Then we show that condition (A.6) is satisfied provided that the initial conditions satisfy (15)–(17). We consider first the case where $-p_1 s_i(D) < v_i(D) \leq -p_2 s_i(D)$. Since $p_1 > p_2$ it follows that the term in the parentheses is non-negative in both (A.2), (A.3). If $0 < v_i(D) \leq -p_1 s_i(D) < -p_2 s_i(D)$, then it holds $v_i(D) + p_2 s_i(D) < v_i(D) + p_1 s_i(D) \leq 0$. Hence, since $e^{(p_2-p_1)(t-D)} \leq 1$ for all $t \geq D$, we obtain

$$v_i(D) + p_2 s_i(D) - e^{(p_2-p_1)(t-D)}(v_i(D) + p_1 s_i(D)) < 0. \tag{A.7}$$

[5]As long as the initial condition for q_i is chosen as $q_i(s) = e^{\Gamma(s+D)}\bar{x}_i(0) + \int_{-D}^{s} e^{\Gamma(s-\theta)}\left(B u_{i0}(\theta) + B_1 u_{i-10}(\theta)\right)d\theta$, $-D \leq s \leq 0$.

In a similar manner, we also get

$$v_i(D) + p_2 s_i(D) - \frac{p_2}{p_1}e^{(p_2-p_1)(t-D)} \times (v_i(D) + p_1 s_i(D)) \leq v_i(D)\left(1 - \frac{p_2}{p_1}\right) < 0, \tag{A.8}$$

for $t \geq D$. Thus, the terms in the parentheses in (A.2), (A.3) are non-negative. Moreover, from (11), (13) it follows that $0 < b \leq -p_2$. Assuming first that $0 < b \leq -p_1 < -p_2$, we obtain $b + p_2 < b + p_1 \leq 0$. Thus, for all $t \in [s, +\infty)$

$$b + p_2 - e^{(p_2-p_1)(t-s)}(b + p_1) < 0. \tag{A.9}$$

In an analogous manner, for $t \in [s, +\infty)$ it holds that

$$b + p_2 - \frac{p_2}{p_1}e^{(p_2-p_1)(t-s)}(b + p_1) \leq b\left(1 - \frac{p_2}{p_1}\right), \tag{A.10}$$

and hence, under (11), which implies $b > 0$, we arrive at

$$b + p_2 - \frac{p_2}{p_1}e^{(p_2-p_1)(t-s)}(b + p_1) < 0. \tag{A.11}$$

If $-p_1 < b \leq -p_2$ then inequalities (A.9), (A.11) still hold. Using (A.7), (A.8), (A.9), and (A.11) we obtain from (A.2)–(A.5) that $s_i(t) > 0$ and $v_i(t) > 0$ for all $t \geq D$, as long as $v_{i-1}(s) > 0$ for $s \geq D$. The latter is true for $i = 1$ by assumption. Thus, by induction in i, we conclude that $s_i(t) > 0$ and $v_i(t) > 0$ for all $t \geq D$ and all $i = 1, 2, \ldots, N$.

We next establish positivity during the dead-time interval and condition (A.6). During the dead-time interval $0 \leq t \leq D$ we have from (2), (3) that

$$\dot{v}_i(t) = u_{i0}(t - D), \tag{A.12}$$

and hence,

$$v_i(t) = v_i(0) + \int_{-D}^{t-D} u_{i0}(s)ds. \tag{A.13}$$

Thus, by assumption (16), it follows that $v_i(t) > 0$ for all $t \in [0, D]$. Using (2) we obtain for $0 \leq t \leq D$

$$\dot{s}_i(t) = v_{i-1}(0) + \int_{-D}^{t-D} u_{i-10}(s)ds - \left(v_i(0) + \int_{-D}^{t-D} u_{i0}(s)ds\right), \tag{A.14}$$

and thus,

$$s_i(t) = s_i(0) + t\,(v_{i-1}(0) - v_i(0)) + \int_{-D}^{t-D}(t - s - D) \times \left(u_{i-10}(s) - u_{i0}(s)\right)ds. \tag{A.15}$$

Thus, under assumption (17), we have $s_i(t) > 0$ for all $t \in [0, D]$. Setting $t = D$ in (A.13), (A.15) we get

$$v_i(D) = v_i(0) + \int_{-D}^{0} u_{i0}(s)ds, \tag{A.16}$$

$$s_i(D) = s_i(0) + D\,(v_{i-1}(0) - v_i(0)) + \int_{-D}^{0} s\left(u_{i0}(s) - u_{i-10}(s)\right)ds. \tag{A.17}$$

Thus, under assumption (15), we conclude using (A.16), (A.17) that condition (A.6) holds.

To prove $\mathcal{L}_p$, $p \in [1,\infty]$, string stability, we capitalize on the specific form (which is a result of predictor-feedback employment) of transfer function

$$G(s) = \frac{V_i(s)}{V_{i-1}(s)}, \quad i = 1, \ldots, N, \tag{A.18}$$

viewing the preceding vehicle's speed as input and the ego vehicle's speed as output, see, e.g., [7] and [13]. Since for homogeneous platoons, under identical feedback laws, we have from (2), (A.18) that (for $i = 2, 3, \ldots, N$) $S_{i-1}(s) = \frac{V_{i-2}(s)-V_{i-1}(s)}{s} = \frac{V_{i-1}(s)}{G(s)}\frac{1-G(s)}{s}$, which implies that $\frac{\Delta_i(s)}{\Delta_{i-1}(s)} = \frac{S_i(s)-hV_i(s)}{S_{i-1}(s)-hV_{i-1}(s)} = \frac{\frac{V_{i-1}(s)-V_i(s)}{s}-hV_i(s)}{S_{i-1}(s)-hV_{i-1}(s)} = G(s)\frac{V_{i-1}(s)-V_i(s)-hsV_i(s)}{V_{i-1}(s)(1-G(s))-hsV_{i-1}(s)G(s)} = G(s)$, it is sufficient to study string stability using G in (A.18). From [10] we have (see also the derivations in Appendix B)

$$G(s) = \frac{bs + \frac{\alpha}{h}}{s^2 + (\alpha + b)\,s + \frac{\alpha}{h}}. \tag{A.19}$$

Since $G(0) = 1$, string stability in $\mathcal{L}_p$, $p \in [1,\infty]$, follows whenever (A.19) corresponds to a non-negative impulse response (see, e.g., [7]). From [23], using (12), (13), the latter holds true when $p_2 < p_1 < 0$, $b > 0$, and $\frac{b}{p_1 p_2} + \frac{1}{p_1} \leq 0$. In turn, these conditions are all satisfied under (10), (11).

Asymptotic stability and zero, steady-state tracking errors for a constant leader's speed, say v^*, follow inductively from estimates (A.2)–(A.5) (starting at $i = 1$ with $v_0 \equiv v^*$ and utilizing the obtained boundedness of each v_i) together with the facts that $\lim_{t\to\infty} v_i(t) = \lim_{t\to\infty} v_{i-1}(t)$ and $\lim_{t\to\infty} s_i(t) = h\lim_{t\to\infty} v_i(t)$, which follow, e.g., using (A.1) and the facts that $\lim_{t\to\infty} \dot{s}_i(t) = \lim_{t\to\infty} \dot{v}_i(t) = 0$ (that, in turn, hold since $r_{1,i}$, $r_{2,i}$ have a finite limit as $t \to \infty$).

Appendix B

Proof of Theorem 2: Existence of $\epsilon_3 > 0$ such that asymptotic stability of individual vehicles is preserved for all $|\Delta D| \in (0, \epsilon_3)$ can be shown using [4], [19], and [21]. We next deal with $\mathcal{L}_2$ string stability robustness. We start deriving (A.18) for $D \neq D_{\rm r}$. Taking Laplace transform of the predictor states (6) we get

$$Q_i(s) = \begin{bmatrix} S_i(s) - DV_i(s) + DV_{i-1}(s) \\ V_i(s) \\ V_{i-1}(s) \end{bmatrix} + M_1(s)U_i(s) + M_2(s)U_{i-1}(s), \tag{B.1}$$

$$M_1(s) = (sI_{3\times3} - \Gamma)^{-1}\left(I_{3\times3} - e^{\Gamma D}e^{-sD}\right)B, \tag{B.2}$$

$$M_2(s) = (sI_{3\times3} - \Gamma)^{-1}\left(I_{3\times3} - e^{\Gamma D}e^{-sD}\right)B_1, \tag{B.3}$$

where we used the fact that

$$e^{\Gamma D} = \begin{bmatrix} 1 & -D & D \\ 0 & 1 & 0 \\ 0 & 0 & 1 \end{bmatrix}.$$

Thus, using (8), (9), we re-write M_1, M_2 term-by-term as

$$M_1(s) = \begin{bmatrix} \frac{e^{-Ds}-1}{s^2} + \frac{De^{-Ds}}{s} \\ \frac{1-e^{-Ds}}{s} \\ 0 \end{bmatrix}, \tag{B.4}$$

$$M_2(s) = \begin{bmatrix} \frac{1-e^{-Ds}}{s^2} - \frac{De^{-Ds}}{s} \\ 0 \\ \frac{1-e^{-Ds}}{s} \end{bmatrix}. \tag{B.5}$$

Using the i-th vehicle's model (2), (20) we have

$$\begin{bmatrix} S_i(s) \\ V_i(s) \end{bmatrix} = \begin{bmatrix} -\frac{1}{s^2} \\ \frac{1}{s} \end{bmatrix} e^{-sD_{\rm r}}U_i(s) + \begin{bmatrix} \frac{1}{s} \\ 0 \end{bmatrix} V_{i-1}(s). \tag{B.6}$$

Combining (5), (B.1), (B.4), and (B.5) we obtain

$$U_i(s) = \frac{\alpha}{h}S_i(s) - \left(\frac{\alpha D}{h} + \alpha + b\right)V_i(s) + \left(\frac{\alpha D}{h} + b\right) \times V_{i-1}(s) + g_1(s)U_i(s) + g_2(s)U_{i-1}(s), \tag{B.7}$$

$$g_1(s) = \frac{\alpha}{h}\left(\frac{e^{-Ds}-1}{s^2} + \frac{De^{-Ds}}{s}\right) - (\alpha + b)\frac{1-e^{-Ds}}{s}, \tag{B.8}$$

$$g_2(s) = -\frac{\alpha}{h}\left(\frac{e^{-Ds}-1}{s^2} + \frac{De^{-Ds}}{s}\right) + b\frac{1-e^{-Ds}}{s}. \tag{B.9}$$

Taking Laplace transform in (20) we get that $e^{-D_{\rm r}s}U_{i-1}(s) = sV_{i-1}(s)$, and hence, substituting (B.6) into (B.7) we arrive at

$$U_i(s) = \left(g_1(s) - \frac{\alpha e^{-sD_{\rm r}}}{hs^2} - \left(\frac{\alpha D}{h} + \alpha + b\right)\frac{e^{-sD_{\rm r}}}{s}\right)U_i(s) + \left(\left(\frac{\alpha D}{h} + b + \frac{\alpha}{hs}\right)\frac{e^{-sD_{\rm r}}}{s} + g_2(s)\right)U_{i-1}(s). \tag{B.10}$$

Therefore, multiplying both sides of (B.10) with $e^{-sD_{\rm r}}$ and using (B.8), (B.9), we write (A.18) as

$$\bar{G}(s) = \frac{bs + \frac{\alpha}{h} + \left(e^{-sD_{\rm r}} - e^{-sD}\right)w_1(s)}{s^2 + (\alpha + b)\,s + \frac{\alpha}{h} + \left(e^{-sD_{\rm r}} - e^{-sD}\right)w_2(s)}, \tag{B.11}$$

$$w_1(s) = \left(b + \frac{\alpha D}{h}\right)s + \frac{\alpha}{h}, \tag{B.12}$$

$$w_2(s) = w_1(s) + \alpha s. \tag{B.13}$$

String stability in $\mathcal{L}_2$ follows if $\left|\bar{G}(j\omega)\right|^2 \leq 1$, $\forall \omega \geq 0$. The condition is satisfied for $\omega = 0$. We next proceed considering first the case $\Delta D = D_{\rm r} - D > 0$. For a given ω, from the mean-value theorem there exist $\xi(\omega)$ and $\zeta(\omega)$ such that

$$\cos(\omega D_{\rm r}) - \cos(\omega D) = -\omega\Delta D\sin(\omega\xi(\omega)), \tag{B.14}$$

$$\sin(\omega D_{\rm r}) - \sin(\omega D) = \omega\Delta D\cos(\omega\zeta(\omega)), \tag{B.15}$$

with $\xi, \zeta \in (D, D_{\mathrm{r}})$. Thus, from (B.11) we have

$$\bar{G}(j\omega) = \frac{f_1(\omega) + jf_2(\omega)}{f_3(\omega) + jf_4(\omega)}, \tag{B.16}$$

$$f_1(\omega) = \frac{\alpha}{h} - \frac{\alpha}{h}\omega\Delta D \sin(\omega\xi(\omega)) + \omega^2\left(\frac{\alpha D}{h} + b\right)\Delta D \cos(\omega\zeta(\omega)), \tag{B.17}$$

$$f_2(\omega) = b\omega - \frac{\alpha}{h}\omega\Delta D \cos(\omega\zeta(\omega)) - \omega^2\left(\frac{\alpha D}{h} + b\right)\Delta D \sin(\omega\xi(\omega)), \tag{B.18}$$

$$f_3(\omega) = -\omega^2 + \alpha\omega^2\Delta D \cos(\omega\zeta(\omega)) + f_1(\omega), \tag{B.19}$$

$$f_4(\omega) = \alpha\omega - \alpha\omega^2\Delta D \sin(\omega\xi(\omega)) + f_2(\omega). \tag{B.20}$$

Therefore, the condition for string stability becomes $f_1(\omega)^2 + f_2(\omega)^2 \leq f_3(\omega)^2 + f_4(\omega)^2$, and hence, after some lengthy but straightforward computations we obtain the following condition that has to hold for all $\omega > 0$

$$\omega^2 f_5(\omega) + \omega f_6(\omega) + \alpha\left(\alpha + 2b - \frac{2}{h}\right) > 0, \tag{B.21}$$

where

$$f_5(\omega) = 1 - 2\left(\alpha + b + \frac{\alpha D}{h}\right)\Delta D \cos(\omega\zeta(\omega)) + \left(\alpha^2 + 2\alpha\left(\frac{\alpha D}{h} + b\right)\right)\Delta D^2 \times \left(\sin(\omega\xi(\omega))^2 + \cos(\omega\zeta(\omega))^2\right), \tag{B.22}$$

$$f_6(\omega) = 2\alpha\left(\frac{1}{h} - \alpha - 2b - \frac{\alpha D}{h}\right)\Delta D \sin(\omega\xi(\omega)). \tag{B.23}$$

As $|\sin(x)| \leq |x|$, $\forall x \in \mathbb{R}$, $\omega > 0$, $\xi > 0$, and $\xi < D_{\mathrm{r}}$ we get

$$f_6(\omega) \geq -2\omega\alpha\left|\frac{1}{h} - \alpha - 2b - \frac{\alpha D}{h}\right|\Delta D(\Delta D + D). \tag{B.24}$$

Since from (B.22) we have that $f_5(\omega) \geq 1 - 2\left(\alpha + b + \frac{\alpha D}{h}\right)\Delta D - 2\left(\alpha^2 + 2\alpha\left(\frac{\alpha D}{h} + b\right)\right)\Delta D^2$, when $\alpha + 2b - \frac{2}{h} > 0$, condition (B.21) holds if

$$-2\left(\alpha + b + \frac{\alpha D}{h}\right)\Delta D - 2\alpha\left(\alpha + 2\left(\frac{\alpha D}{h} + b\right)\right)\Delta D^2 - 2\alpha\left|\frac{1}{h} - \alpha - 2b - \frac{\alpha D}{h}\right|\Delta D(\Delta D + D) + 1 > 0. \tag{B.25}$$

The left-hand side of (B.25) is a continuous function of ΔD and equal to unity when $\Delta D = 0$. Thus, there exists a sufficiently small $\epsilon_1 > 0$ such that for all $0 < \Delta D < \epsilon_1$ the left-hand side of (B.25) is positive, which completes the proof for $\Delta D > 0$. In the exact same manner one can treat the case $\Delta D < 0$. In particular, one arrives at the following, almost identical to (B.25), condition

$$1 + 2\left(\alpha + b + \frac{\alpha D}{h}\right)\Delta D - 2\left(\alpha^2 + 2\alpha\left(\frac{\alpha D}{h} + b\right)\right) \times \Delta D^2 + 2D\alpha\left|\frac{1}{h} - \alpha - 2b - \frac{\alpha D}{h}\right|\Delta D > 0. \tag{B.26}$$

Condition (B.26) can be satisfied for all $0 < -\Delta D < \epsilon_2$, for a sufficiently small $\epsilon_2 > 0$. The proofs of stability and string stability robustness are completed with $\epsilon = \min\{\epsilon_1, \epsilon_2, \epsilon_3\}$.

We next show that zero steady-state error is achieved. Since each individual vehicular system is stable, which also implies that all poles of $\bar{G}$ have negative real parts (see, e.g., Corollary 2.3 in [19]), we have for some constant speed for the leading vehicle, say v^*, $\lim_{t\to+\infty} v_i(t) = \lim_{s\to 0} s\frac{v^*}{s}\bar{G}(s)^i$ (see, e.g., [9]), and hence, using (B.11) we get $\lim_{t\to+\infty} v_i(t) = v^*\bar{G}(0)^i = v^*$. Moreover, we have $S_i(s) = \frac{V_{i-1}(s) - V_i(s)}{s} = V_{i-1}(s)\frac{1-\bar{G}(s)}{s} = \frac{v^*}{s}\bar{G}(s)^{i-1}\frac{1-\bar{G}(s)}{s}$. Re-writing $\bar{G}$ as $\bar{G}(s) = \frac{n(s)}{d(s)}$, we get $\frac{1-\bar{G}(s)}{s} = \frac{d(s)-n(s)}{sd(s)}$, which has no pole at the origin, since from (B.11)–(B.13) it follows that $d(s) - n(s) = s^2 + \alpha s + \left(e^{-sD_{\mathrm{r}}} - e^{-sD}\right)\alpha s$, and hence, $\frac{d(s)-n(s)}{sd(s)} = \frac{s+\alpha+\left(e^{-sD_{\mathrm{r}}} - e^{-sD}\right)\alpha}{d(s)}$ (and all roots of d have negative real parts). Thus, $\lim_{t\to+\infty} s_i(t) = \lim_{s\to 0} sS_i(s) = \lim_{s\to 0} s\frac{v^*}{s}\bar{G}(s)^{i-1}\frac{s+\alpha+\left(e^{-sD_{\mathrm{r}}} - e^{-sD}\right)\alpha}{d(s)} = hv^*$.

REFERENCES

[1] I. Abel, M. Jankovic, and M. Krstić, "Constrained stabilization of multi-input linear systems with distinct input delays," *IFAC-PapersOnLine*, vol. 52, no. 2, pp. 82–87, 2019.

[2] L. Alvarez and R. Horowitz, "Safe platooning in automated highway systems Part I: Safety regions design," *Vehicle Syst. Dyn.*, vol. 32, no. 1, pp. 23–55, Jul. 1999.

[3] A. D. Ames, X. Xu, J. W. Grizzle, and P. Tabuada, "Control barrier function based quadratic programs for safety critical systems," *IEEE Trans. Autom. Control*, vol. 62, no. 8, pp. 3861–3876, Aug. 2017.

[4] N. Bekiaris-Liberis and M. Krstic, *Nonlinear Control Under Nonconstant Delays*. Philadelphia, PA, USA: SIAM, 2013.

[5] N. Bekiaris-Liberis and M. Krstic, "Predictor-feedback stabilization of multi-input nonlinear systems," *IEEE Trans. Autom. Control*, vol. 62, no. 2, pp. 516–531, Feb. 2017.

[6] N. Bekiaris-Liberis, C. Roncoli, and M. Papageorgiou, "Predictor-based adaptive cruise control design," *IEEE Trans. Intell. Transp. Syst.*, vol. 19, no. 10, pp. 3181–3195, Oct. 2018.

[7] A. Bose and P. A. Ioannou, "Analysis of traffic flow with mixed manual and semiautomated vehicles," *IEEE Trans. Intell. Transp. Syst.*, vol. 4, no. 4, pp. 173–188, Dec. 2003.

[8] C. C. de Wit and B. Brogliato, "Stability issues for vehicle platooning in automated highway systems," in *Proc. IEEE Int. Conf. Control Appl.*, Kohala Coast, HI, USA, vol. 2, Aug. 1999, pp. 1377–1382.

[9] J. Chen, K. H. Lundberg, D. E. Davison, and D. S. Bernstein, "The final value theorem revisited: Infinite limits and irrational functions," *IEEE Control Syst. Mag.*, vol. 27, no. 3, pp. 97–99, Jun. 2007.

[10] L. C. Davis, "Method of compensation for the mechanical response of connected adaptive cruise control vehicles," *Phys. A, Stat. Mech. Appl.*, vol. 562, Jan. 2021, Art. no. 125402.

[11] L. C. Davis, "Stability of adaptive cruise control systems taking account of vehicle response time and delay," *Phys. Lett. A*, vol. 376, nos. 40–41, pp. 2658–2662, Aug. 2012.

[12] L. Farina and S. Rinaldi, *Positive Linear Systems: Theory and Application*. Hoboken, NJ, USA: Wiley, 2000.

[13] J. I. Ge and G. Orosz, "Dynamics of connected vehicle systems with delayed acceleration feedback," *Transp. Res. C, Emerg. Technol.*, vol. 46, pp. 46–64, Sep. 2014.

[14] G. Gunter et al., "Are commercially implemented adaptive cruise control systems string stable?" *IEEE Trans. Intell. Transp. Syst.*, vol. 22, no. 11, pp. 6992–7003, Nov. 2021.

[15] C. R. He and G. Orosz, "Safety guaranteed connected cruise control," in *Proc. 21st Int. Conf. Intell. Transp. Syst. (ITSC)*, Maui, HI, USA, Nov. 2018, pp. 549–554.

[16] S. Huang and W. Ren, "Autonomous intelligent cruise control with actuator delays," *J. Intell. Robot. Syst., Theory Appl.*, vol. 23, no. 1, pp. 27–43, 1998.
[17] M. Jankovic, "Control barrier functions for constrained control of linear systems with input delay," in *Proc. Annu. Amer. Control Conf. (ACC)*, Jun. 2018, pp. 3316–3321.
[18] L. Juárez and S. Mondié, "Dynamic predictor-based extended cooperative adaptive cruise control," in *Proc. IFAC Workshop Time Delay Syst.*, 2019, pp. 7–12.
[19] I. Karafyllis and M. Krstic, "Delay-robustness of linear predictor feedback without restriction on delay rate," *Automatica*, vol. 49, no. 6, pp. 1761–1767, Jun. 2013.
[20] I. Karafyllis, D. Theodosis, and M. Papageorgiou, "Nonlinear adaptive cruise control of vehicular platoons," *Int. J. Control*, vol. 96, no. 1, pp. 147–169, Jan. 2023.
[21] M. Krstic, "Lyapunov tools for predictor feedbacks for delay systems: Inverse optimality and robustness to delay mismatch," *Automatica*, vol. 44, no. 11, pp. 2930–2935, 2008.
[22] C.-Y. Liang and H. Peng, "String stability analysis of adaptive cruise controlled vehicles," *JSME Int. J. C, Mech. Syst., Mach. Elements Manuf.*, vol. 43, no. 3, pp. 671–677, 2000.
[23] S. Lin and C.-J. Fang, "Nonovershooting and monotone nondecreasing step responses of a third-order SISO linear system," *IEEE Trans. Autom. Control*, vol. 42, no. 9, pp. 1299–1303, Sep. 1997.
[24] X. Liu, A. Goldsmith, S. S. Mahal, and J. K. Hedrick, "Effects of communication delay on string stability in vehicle platoons," in *Proc. IEEE Intell. Transp. Syst.*, Oakland, CA, USA, Aug. 2001, pp. 625–630.
[25] T. G. Molnár, W. B. Qin, T. Insperger, and G. Orosz, "Application of predictor feedback to compensate time delays in connected cruise control," *IEEE Trans. Intell. Transp. Syst.*, vol. 19, no. 2, pp. 545–559, Feb. 2018.
[26] T. G. Molnar, A. K. Kiss, A. D. Ames, and G. Orosz, "Safety-critical control with input delay in dynamic environment," 2021, *arXiv:2112.08445*.
[27] G. Orosz, R. E. Wilson, and G. Stépán, "Traffic jams: Dynamics and control," *Philos. Trans. Roy. Soc. A*, vol. 368, no. 1928, pp. 4455–4479, 2010.
[28] J. Ploeg, N. van de Wouw, and H. Nijmeijer, "$\mathcal{L}_p$ string stability of cascaded systems: Application to vehicle platooning," *IEEE Trans. Control Syst. Technol.*, vol. 22, no. 2, pp. 786–793, Mar. 2014.
[29] R. Rajamani, *Vehicle Dynamics and Control*. New York, NY, USA: Springer, 2006.
[30] R. Rajamani and S. E. Shladover, "An experimental comparative study of autonomous and co-operative vehicle-follower control systems," *Transp. Res. C, Emerg. Technol.*, vol. 9, no. 1, pp. 15–31, Feb. 2001.
[31] R. Sipahi and S. I. Niculescu, "Deterministic time-delayed traffic flow models: A survey," in *Complex Time-Delay Systems*, F. M. Atay, Ed. Berlin, Germany: Springer, 2010.
[32] A. Schwab and J. Lunze, "Design of platooning controllers that achieve collision avoidance by external positivity," *IEEE Trans. Intell. Transp. Syst.*, vol. 23, no. 9, pp. 14883–14892, Sep. 2022.
[33] D. Swaroop and J. K. Hedrick, "String stability of interconnected systems," *IEEE Trans. Autom. Control*, vol. 41, no. 3, pp. 349–357, Mar. 1996.
[34] M. Wang, S. P. Hoogendoorn, W. Daamen, B. van Arem, B. Shyrokau, and R. Happee, "Delay-compensating strategy to enhance string stability of autonomous vehicle platoons," in *Proc. Transp. Res. Board 95th Annu. Meeting*, 2016.
[35] L. Xiao and F. Gao, "Practical string stability of platoon of adaptive cruise control vehicles," *IEEE Trans. Intell. Transp. Syst.*, vol. 12, no. 4, pp. 1184–1194, Dec. 2011.
[36] H. Xing, J. Ploeg, and H. Nijmeijer, "Smith predictor compensating for vehicle actuator delays in cooperative ACC systems," *IEEE Trans. Veh. Technol.*, vol. 68, no. 2, pp. 1106–1115, Feb. 2019.
[37] H. Xing, J. Ploeg, and H. Nijmeijer, "Compensation of communication delays in a cooperative ACC system," *IEEE Trans. Veh. Technol.*, vol. 69, no. 2, pp. 1177–1189, Feb. 2020.
[38] D. Yanakiev and I. Kanellakopoulos, "Longitudinal control of automated CHVs with significant actuator delays," *IEEE Trans. Veh. Technol.*, vol. 50, no. 5, pp. 1289–1297, Sep. 2001.
[39] L. Zhang and G. Orosz, "Motif-based design for connected vehicle systems in presence of heterogeneous connectivity structures and time delays," *IEEE Trans. Intell. Transp. Syst.*, vol. 17, no. 6, pp. 1638–1651, Jun. 2016.
[40] Y. Zhang, Y. Bai, J. Hu, and M. Wang, "Control design, stability analysis, and traffic flow implications for cooperative adaptive cruise control systems with compensation of communication delay," *Transp. Res. Rec., J. Transp. Res. Board*, vol. 2674, no. 8, pp. 638–652, Aug. 2020.
[41] Y. Zhang, Y. Bai, M. Wang, and J. Hu, "Cooperative adaptive cruise control with robustness against communication delay: An approach in the space domain," *IEEE Trans. Intell. Transp. Syst.*, vol. 22, no. 9, pp. 5496–5507, Sep. 2021.
[42] Y. Zheng, S. E. Li, K. Li, F. Borrelli, and J. K. Hedrick, "Distributed model predictive control for heterogeneous vehicle platoons under unidirectional topologies," *IEEE Trans. Control Syst. Technol.*, vol. 25, no. 3, pp. 899–910, Dec. 2017.

Nikolaos Bekiaris-Liberis (Member, IEEE) received the Ph.D. degree in aerospace engineering from the University of California at San Diego, San Diego, USA, in 2013. From 2013 to 2014, he was a Post-Doctoral Researcher with the University of California at Berkeley, Berkeley, USA. From 2019 to 2022, he was an Assistant Professor, from 2017 to 2019, he was a Marie Sklodowska-Curie Fellow, and from 2014 to 2017, he was a Research Associate with the Technical University of Crete, Greece, where he is currently an Associate Professor with the Department of Electrical and Computer Engineering. He has authored/coauthored one book and more than 100 papers. His research interests include nonlinear delay, switched, and distributed parameter systems, and their applications to transport systems. He received the Chancellor's Dissertation Medal in Engineering from the University of California at San Diego in 2014 and the George N. Saridis Outstanding Research Paper Award in 2019. He was a recipient of the 2016 Marie Sklodowska-Curie Individual Fellowship Grant and he received a 2022 European Research Council (ERC) Consolidator Grant.